Canadian Geotechnical Journal

Research Article

Effect of sodium occupancy and solute concentration on the swelling pressure and hydraulic conductivity of Boom Clay

Hassan Al Mais[a,b,c], **Yu-Jun Cui**[c], **Xiang-Ling Li**[d], **Suresh Seetharam**[a], **Elie Valcke**[a], **Lian Wang**[a], **Temenuga Georgieva**[d], **and Frédéric Collin**[b]

[a]SCK CEN, Mol, Belgium; [b]Université de Liège, Liège, Belgium; [c]Ecole Nationale des Ponts et Chaussées (ENPC), Navier Laboratory/CERMES, Marne La Vallée, France; [d]EURIDICE, Mol, Belgium

Corresponding author: **Yu-Jun Cui** (email: yu-jun.cui@enpc.fr)

Abstract

The poorly indurated Boom Clay (BC) has been studied as a potential host formation for the geological disposal of radioactive waste including the intermediate-level long-lived bituminized radioactive waste called Eurobitum. In case of leaching of Eurobitum, fluids with altered chemical compositions would be expected to infiltrate locally into the BC. To evaluate the effect of salinity on the BC hydromechanical behaviour, a series of one-dimensional constant-volume swelling tests were conducted on intact BC samples that were first percolated with mixed sodium-calcium-nitrate solutions ((Na, Ca)NO_3) with varying sodium concentrations, resulting in varying Na^+ occupancies in the clay. Results showed that the swelling pressure of BC decreased with an increase in the solute concentration and sodium occupancy. Additionally, higher Na^+ concentrations led to a faster stabilization of the swelling pressure. The hydraulic conductivity of BC increased with increasing solute concentration and sodium occupancy. Moreover, the sodium occupancy and concentration affected the swelling pressure and hydraulic conductivity in a similar way. This phenomenon could be elucidated by two primary mechanisms: (i) the influence of solute concentration on the diffuse double layer, and (ii) the effect of cation type and hydrated radius within the interbasal space of montmorillonite sheets, especially concerning sodium occupancy.

Key words: Boom Clay, swelling behaviour, concentration, occupancy, diffuse double layer, hydrated cation radius

1. Introduction

In many countries, deep geological disposal is a widely adopted option for the long-term management of intermediate-level and high-level long-lived radioactive waste (McCombie 2005; Push 2008; Chapman and Hooper 2012). Most designs of deep underground repositories are based on the multibarrier principle, encompassing metallic waste containers, engineered barriers (positioned around the waste containers), and a natural barrier (host formation) (Li et al. 2023). In Belgium, the Boom Clay (BC), a poorly indurated clay, has been identified as a potential host formation for radioactive waste disposal. This selection is driven by the favourable characteristics such as low permeability, high radionuclide retention/sorption properties, and good self-sealing capacity (De Craen et al. 2004). This study focuses on a specific intermediate-level waste form of importance to Belgium, referred to as Eurobitum, which is a bituminized radioactive waste (BW) that mainly incorporates precipitation sludges originating from the chemical reprocessing of spent nuclear fuel. A key feature of Eurobitum is that besides the bitumen, it contains large amounts of $NaNO_3$ (mostly between 20 and 30 wt.%), $CaSO_4$ (mostly between 4 and 6 wt.%), and other chemicals such as CaF_2, $Ca_3(PO_4)_2$, etc. (Valcke et al. 2009). Final disposal in a clay host rock is one of the long-term management options considered for this waste. The current disposal concept foresees that several primary 220 L waste packages would be emplaced in a secondary thick-walled concrete disposal container with mortar backfilling in the void space. The containers would then be placed in disposal galleries lined with concrete and the void space between the two systems would be backfilled with mortar. Over time, the engineered barriers, composed of cementitious materials with a high concentration of hyperalkaline components, are expected to become saturated due to the seepage and diffusion of water originating from the clay formation through the porous barrier materials. After the closure of the disposal galleries, contact between the BW and hyperalkaline water from the surrounding saturated cementitious barriers will lead to water uptake and osmosis-induced expansion of the waste (Valcke et al. 2009). Subsequently, amongst others, Na(NO_3, NO_2) and $CaSO_4$, will leach out of the waste and diffuse through the cementitious engineered barriers towards the host clay formation, along with the Na^+, K^+, Ca^{2+}, and OH^- in the hyperalkaline pore

water. If the combined BW salts and alkaline plume reaches the host clay formation, it may lead to locally elevated salt concentrations in the clay pore water, which may affect the hydro-mechanical behaviour of a small layer (up to ~3 m; Weetjens et al. 2010; Bleyen et al. 2018) of BC surrounding the engineered barrier system. In addition, interaction of this nearby BC with these plumes may impact its performance by potentially changing the aforementioned favourable properties. It is therefore of interest to better understand the chemo-hydro-mechanical process and to quantify the effect of the saline plume on the hydro-mechanical response of BC, in particular, in terms of swelling pressure and hydraulic conductivity.

The impact of pore fluid composition on clay behaviour has gained substantial attention in different fields, including clay mineralogy (Low 1980), soil physics (Barshad 1952; Sposito 1981), geotechnical engineering (Bolt 1956; Mesri and Olson 1971; Sridharan and Rao 1973), and environmental engineering (Ye et al. 2014). The hydro-mechanical behaviour of clays can be influenced by the salinity of pore water (Studds et al. 1998; Di Maio et al. 2004; Rao and Thyagaraj 2007; Agus et al. 2013).

A great number of experimental studies addressing the chemical influences on clay swelling behaviour are documented in the literature (Studds et al. 1998; Calvello et al. 2005; Ye et al. 2014). These studies highlight that increased pore water salinity can significantly decrease the swelling pressure (Komine et al. 2009; Zhu et al. 2013) while simultaneously increasing the hydraulic conductivity (Castellanos et al. 2008; Zhu et al. 2013). Yukselen-Aksoy et al. (2008) and Zhu et al. (2013) noted that some cations in the pore water, like sodium and potassium, may induce alteration in mineralogical composition through cation exchange in the interlayer space of montmorillonite sheets, influencing the crystalline swelling process and resulting in lower swelling pressure. Additionally, depending on the initial conditions, both ionic strength (IS) and ion exchange of adsorbed cations with cations present in the pore water can reduce the thickness of the diffuse double layer (DDL), impacting the osmotic swelling behaviour (Castellanos et al. 2008; Schanz and Tripathy 2009; Siddiqua et al. 2011; Zhu et al. 2013; Du et al. 2021).

Moreover, increasing pore water salt concentration weakens the repulsion forces of the DDL, thereby reducing the swelling potentials (Calvello et al. 2005). A consistent observation across various studies is that salt solutions induce structural collapse in clay, decrease the thickness of the DDL, elevate hydraulic conductivity, and diminish swelling potential. Simons and Reuter (1985), Evans and Quigley (1992), and Di Maio (1996) investigated the interplay between leaching, chemical changes, and clay behaviour. Changes in the chemical composition of clay pore water may result in some effects across microscopic, mesoscopic, and macroscopic scales. These effects include the exchange of positively charged ions among mineral components, fluctuations in electrochemical forces of the DDL, increase in osmotic pressure, and exchange of cations between clay sheets and particles. Essentially, alterations in pore fluid chemistry may influence the characteristics of clay across various observation levels, such as the cation exchange capacity (CEC) and cation occupancy. The CEC corresponds to the quantity of exchangeable cations at a given pH, traditionally measured in milliequivalents (meq)/100 g of calcined clay (Bergaya and Vayer 1997). A parallel definition was put forth by Środoń and McCarty (2008), who elaborated that the CEC of a soil denotes the cumulative cations available for exchange held across the entire specific surface area of soil. The CEC is an important parameter influencing the retention and retardation of radionuclides within a clay formation for the geological disposal of radioactive waste (Honty 2010). The adsorbed cations on the clay surface can be exchanged with cations in the pore water in such a way that the electroneutrality of both the solid and the solution is preserved. Honty (2010) reported a range from 130 ± 33 to 270 ± 20 meq.kg^{-1} for the CEC of BC at the reference site Mol-Dessel. The average CEC value reported by Frederickx et al. (2018), based on the BC samples extracted from the HADES underground laboratory level, is of 222 ± 33 meq.kg^{-1} on average. The CEC variations depend on the smectite content (which contributes to ~90% of CEC).

Cation occupancy refers to the proportion or fraction of a specific cation over the total amount of exchangeable cations. It indicates the degree to which a clay is filled by this cation compared to the total number of adsorbed cations. Cation occupancy can have significant impact on the physical, chemical, and mechanical properties of minerals, particularly in clay minerals and other crystalline structures that involve ion exchange and interactions with surrounding solutions (Yotsuji et al. 2021). Regarding the cation occupancies in undisturbed BC, Wang et al. (2023) reported that the main cations are Na^+, K^+, Mg^{2+}, and Ca^{2+}. Their values vary as function of the Na^+ concentration in the clay pore water, which increases with depth. The average cation occupancies were found to be approximately Na (22%–47%), K (8%–19%); Mg (20,%–40%), and Ca (20%–40%).

Although there are numerous studies examining the influence of cation valence on ion exchange reactions during the percolation of saline solutions, investigations into the effect of hydrated radius and cation type on saturated clay swelling and hydraulic conductivity are limited. Furthermore, to date, very few studies (Mokni 2011; Bleyen et al. 2018) exist concerning the impact of saline plume originating from the bituminized waste on the physico-chemical and hydro-mechanical behaviour of BC. This paper therefore presents an investigation of the impact of the sodium occupancy and of the solute concentration on the swelling behaviour and hydraulic conductivity of BC. One-dimensional swelling pressure tests were conducted on intact samples, which were first percolated with either a $NaHCO_3$ solution simulating the in situ porewater composition, or with (Na, Ca)NO_3 solutions of different concentrations (total concentrations of 1 and 2 mol/L) and Na/Ca ratios, defining different Na+ occupancies of 10%, 20%, 60%, or 90%. The percolation was carried out using an oedometer frame at the vertical effective in situ stress of 2.25 MPa, after which the oedometer cell was instantaneously moved to a constant volume cell to investigate the swelling pressure and hydraulic conductivity. More details can be found in Section 2.3.

Table 1. Composition of saline solutions.

Solution	Na^+—Occupancy (%)	$NaNO_3$ (mmol/L)	$Ca(NO_3)_2$ (mmol/L)	Ionic strength (mol/L)	Pore volume (PV)
1	60%	900	70	1.0	3
2	60%	1600	230	2.0	6
3	90%	2000	–	2.0	5
4	20%	320	340	1.0	3
5	10%	165	400	1.0	3

The higher occupancies (60% and 90%) simulate the response of the BC to the saline plume identified by coupled geochemical and transport simulations (see further) regarding the leaching of salt from the bituminized waste, while the lower occupancies (10% and 20%) were included to cover the range of Na^+ occupancies for comparison purposes. Based on the test results, the effects of solution concentration and sodium occupancy on the swelling potential and hydraulic conductivity are discussed. It is important to note that this study focuses solely on the effect of saline solutions, without considering the influence of alkalinity or pH, even though pH can greatly affect the hydro-mechanical behaviour of BC.

2. Materials and methods

2.1. Materials

The material studied is the BC obtained during coring campaigns in the HADES underground research laboratory (URL) at Mol. The cores were 90–100 mm in diameter and 600–1000 mm in length. The cores were taken from a horizontal borehole, oriented normal to the bedding plane, and were vacuum-wrapped in thermo-welded reinforced aluminium foil to limit water desaturation. Samples were prepared from two different cores: the initial core is denoted as R78-79 W_Core 28.1, while the subsequent core is referenced as R78-79 W_Core 2. The former is located at approximately 28.1 m horizontally from the Connecting Gallery at the HADES underground laboratory level, representing the intact BC, while the latter is situated at 2.2 m away, within the excavation damaged zone of the main HADES URL gallery. All cores were waxed and stored in a hermetically sealed chamber at a temperature of 20 °C and a relative humidity of approximately 99%.

To span a large domain of Na^+ occupancies and solution concentrations, five different saline solutions with varying total concentration, Na^+ and Ca^{2+} concentration, and ratios were considered, in comparison with the pore water chemistry of intact BC. Only Na^+ and Ca^{2+} were considered in this study (see Table 1). The sodium occupancy can be determined using eq. 1, where the ion concentration is divided by the total CEC of the clay. The IS is calculated using eq. 2, where c_i represents the ion concentration and z_i represents the ion charge. The higher Na^+ occupancies (60% and 90%) and total concentrations (1 and 2 mol/L) are deduced from the work of Weetjens et al. (2010), who modeled, by means of combined geochemical and transport calculations, the expected evolution of the Na^+ concentration and Na^+ occupancy for a hypothetical disposal of Eurobitum in the BC. Ten percent and 20% were arbitrarily chosen for the lower Na^+ occupancies with a 1 mol/L total concentration. Additionally, a natural system with a Na^+ occupancy of approximately 30%, representing the initial sodium occupancy in the clay materials of BC (Honty 2010) in contact with 15 mmol/L $NaHCO_3$, was included. The most recent study done by Honty et al. (2022), through the experimental investigation of BC pore water chemistry, reveals that present-day BC pore water is a dilute $NaHCO_3$ solution ranging from 10 to 20 mmol/L, with a value of alkaline pH slightly higher than 8.

Table 1 represents the concentration and composition of each solution consisting of sodium nitrate ($NaNO_3$) and calcium nitrate ($Ca(NO_3)_2$). Additionally, a synthetic BC solution with a sodium bicarbonate ($NaHCO_3$) concentration of 15 mmol/L (simulating intact BC pore water chemistry as recommended by De Craen et al. 2004), was investigated as a reference for comparison purposes. It is worth noting that the cation occupancy refers to the total contribution of a specific cation to the overall exchangeable cations in the clay material. For instance, a 90% sodium occupancy implies that 90% of the exchangeable cations in the sample are sodium, while the remaining 10% consist of magnesium, calcium, potassium, and other elements.

$$(1)\quad \text{occupancy (\%)} = \frac{\text{concentration of exchangeable cation}}{\text{CEC}} \times 100$$

$$(2)\quad \text{IS} = \frac{1}{2}\sum_{i=1}^{n} c_i z_i^2$$

where c_i represents the ion concentration and z_i represents the ion charge.

2.2. Sample preparation

The BC is an anisotropic clay. The orientation of bedding planes is visible to the naked eye immediately after the plastic bag with the core is opened. Regarding the preparation of samples for swelling pressure and hydraulic conductivity measurements, the core was divided into four slices, each 20 mm thick (see Fig 1*a*). Subsequently, manual trimming was carried out using a sharp blade cutter and a cutting ring (Figs. 1*b* and 1*c*) to prepare a sample with a diameter of 50 mm and a height of 10 mm (Fig. 1*d*). Special attention was paid to preserving the initial water content. The preservation process involved wrapping the samples with Parafilm made of

Fig. 1. Sample preparation for swelling pressure test.

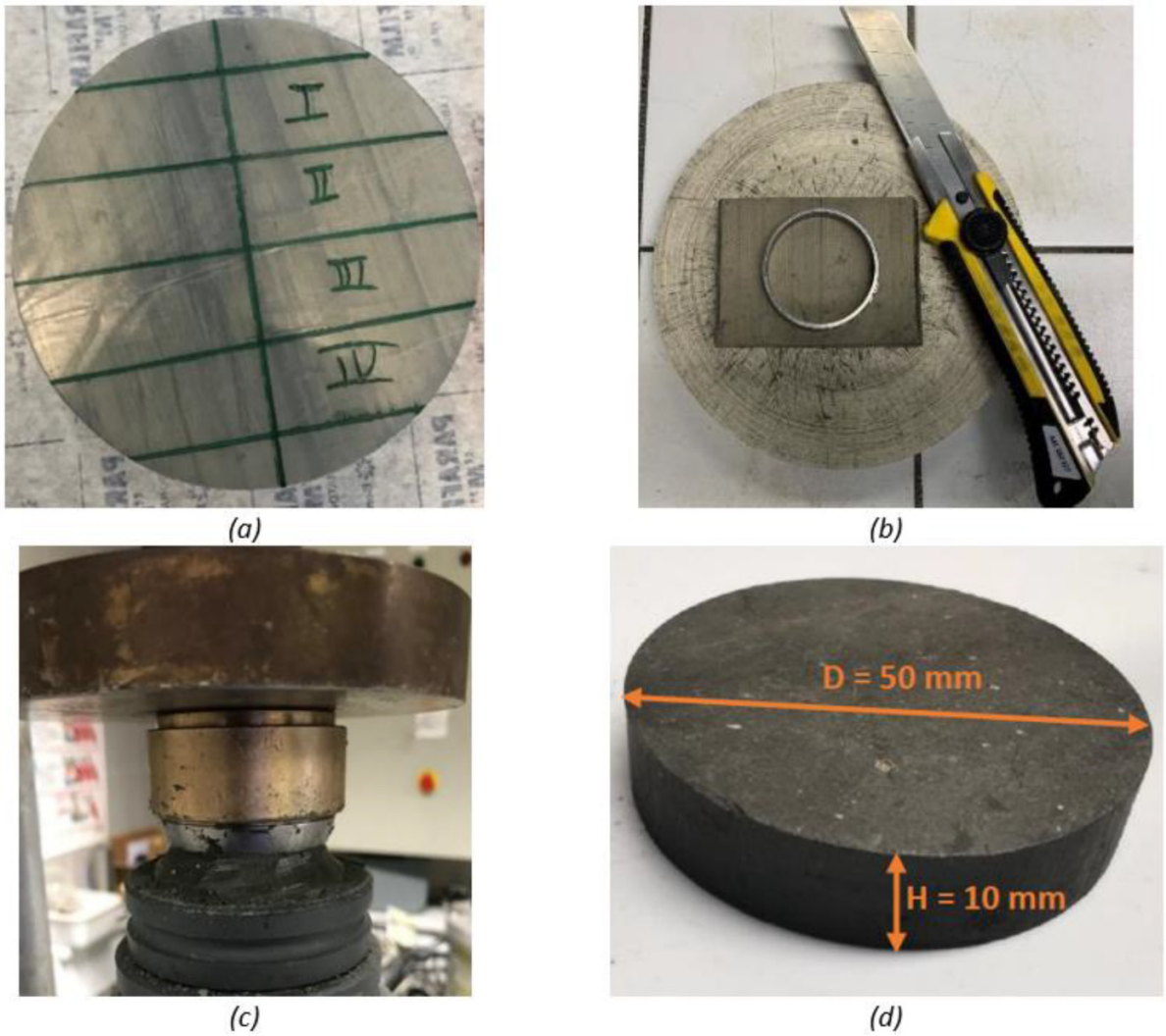

wax blends, followed by placing them in high-density vacuum storage bags, and finally, vacuum-packing them using a fast vacuum (Awarkeh 2023). Table 2 presents the main characteristics of all the samples. It can be observed that the water content is in the range 20% < w_0 < 23%, and the saturation is in the range 93% < S_r < 100%. Note that the specific solid density (Gs) used for BC in this study is 2.65 Mg/m^3 (De Craen et al. 2004). The void ratio was calculated based on the bulk density of the grain solids, as well as the total volume and mass of each sample. Since the samples were hand-trimmed and prepared from different cores, which may have some heterogeneities, these variations—along with differences in water content and clay content—could affect the initial void ratio. It can be observed that the initial void ratio of the tested samples varied between 0.554 and 0.605. To minimize the impact of heterogeneities between samples, each sample was percolated with different salt solutions to test the effect of sodium occupancy and solute concentration.

The loading direction was chosen to be normal to the bedding plane.

2.3. Experimental set-up and test program

Per test condition the swelling pressure measurement and the hydraulic conductivity measurement were done on the same BC sample. All the tests were performed at a controlled temperature of 20 ± 1 °C.

2.3.1. Swelling pressure

Before conducting the swelling pressure test, the sample was carefully positioned inside an oedometer cell, sandwiched between two dry metallic porous disks covered with filter papers at the top and bottom. To reduce lateral surface friction, the interior of the cell wall was coated with grease. The oedometer cell was equipped with two valves in its base to facilitate saturation of the porous discs, while vertical drainage was permitted through the top porous disks.

The sample was loaded stepwise up to the in situ effective stress of 2.25 MPa. Afterwards, saturation was carried out using the desired solution and an infiltration cell connected to a controller of pressure and volume (CPV). To achieve the desired Na^+ occupancies of 60% at 1.0 mol/L, 60% at 2.0 mol/L,

Table 2. Geometry, initial water content, and initial void ratio for the specimens tested.

Test	Sample localization	D_0 (mm)	H_0 (mm)	ρ (g/cm^3)	W_0 (%)	e_0	S_r
1	R78-79 W_Core 28.1 Block5-SliceI	49.11	10.00	2.07	22.6	0.565	1.00
2	R78-79 W_Core 28.1 Block5-SliceIII	49.90	9.90	2.02	20.0	0.565	0.93
3	R78-79 W_Core 2.2 Block2-SliceIII	49.90	9.92	2.06	21.0	0.554	1.00
4	R78-79 W_Core 2.2 Block3-SliceIII	49.86	10.07	2.03	22.3	0.595	0.99
5	R78-79 W_Core 28.1 Block6-SliceII	49.66	9.89	2.04	21.7	0.575	0.99
6	R78-79 W_Core 28.1 Block5-SliceIV	49.76	9.95	2.04	23.63	0.603	1.00
7	R78-79 W_Core 28.1 Block6-SliceI	49.83	9.75	2.03	23.43	0.605	1.00
8	R78-79 W_Core 28.1 Block9-SliceI	49.90	9.78	2.04	21.7	0.576	0.99
9	R78-79 W_Core 28.1 Block9-SliceII	49.86	9.99	2.04	20.8	0.569	0.97

and 90% at 2.0 mol/L, a percolation of 3, 6, and 5 times the pore volume of the sample was applied. The required number of pore volume replacements was obtained from geochemical calculations using a geochemical computer code (Weetjens et al. 2010). For solutions with 20% and 10% sodium occupancies and 1.0 mol/L concentration, 3 pore volumes were enough, as these solutions contain a high amount of calcium, and less pore volume replacements were required to achieve the desired sodium occupancy due to the easier replacement of the divalent cation Ca^{2+} versus the monovalent cation Na^{+} (Mitchell and Soga 2005). Once the specified percolated volume was achieved, the saturation phase was deemed completed. For the BC synthetic solution (15 mmol/L $NaHCO_3$), a minimum of two times the pore volume was percolated to ensure thorough sample saturation.

After saturation, excess water from the saturation phase was removed from the cell by air flushing, and the sample was rapidly unloaded and transferred to the constant-volume cell to initiate the swelling pressure test (Fig. 2). During this transfer process, negative internal suction developed, maintaining the sample volume almost constant. This behaviour was proved by sacrificing several tests after the saturation phase and fast unloading, during which the total suction induced by the fast unloading was measured using a chilled-mirror dew-point hygrometer (WP4) (Ying et al. 2021). The "stress release suction" refers to the suction generated by the rapid unloading without water supply. In this process, the clay undergoes a sudden reduction of external pressure while its volume remains constant due to the stress release suction (Le et al. 2011; Zhang et al. 2022; Yang et al. 2024). Table 3 presents the measured total suction and the osmotic suction related to the (Na, Ca)NO_3 concentration for the three main solutions (BC synthetic solution, 1.0 and 2.0 mol/L), calculated using the equation proposed by Beyer and Steiger (2002). The difference between the measured total suction by WP4 and the calculated osmotic suction leads to the suction due to the fast unloading of the BC sample without contact with water, referred to as the stress release suction (Zhang et al. 2022; Yang et al. 2024). Notably, an internal negative stress release suction of approximately 3.5 MPa was observed for the BC synthetic solution, which is quite high. For solutions with Na = 60% and IS = 1.0 mol/L, and Na = 90% and IS = 2.0 mol/L, the released stress release suctions were found to be 4.25 and 5 MPa, respectively. It is clear that the measured total suction increases with the increasing solution concentration, which is mainly attributed to the increase in osmotic suction.

Once the oedometer cell was properly placed in the constant-volume cell (Zeng et al. 2019), the first desired solution from a reservoir was percolated under low pressure (50 kPa) into the first valve at the base of the cell to evacuate any air, and then the second valve was closed as water started to flow out. The swelling pressure was measured by the force transducer installed at the bottom of cell and was recorded by a data logging system. In this procedure, the injection pressure was gradually raised until a stable pressure (100 kPa), regulated by the CPV. This pressure was maintained between the upper and lower sections of the sample throughout the test. To minimize the disturbance to the microstructure and to prevent hydraulic fracturing, the water injection pressure was intentionally kept below 1/10 of the ultimate swelling pressure. When the recorded swelling pressure was stable for 48 h, the test was considered as completed. Afterwards, the hydraulic conductivity was determined.

2.3.2. Hydraulic conductivity

To determine the saturated hydraulic conductivity, the constant hydraulic head method was employed. The CPV monitored and recorded the injected solution volume. The test was terminated when the volume of injected solution was equal to that necessary for replacing the desired number of pore volumes for each solution.

Subsequent to the injection test, the injection pressure was decreased to 50 kPa, allowing assessment of the impact

Fig. 2. Constant-volume cell.

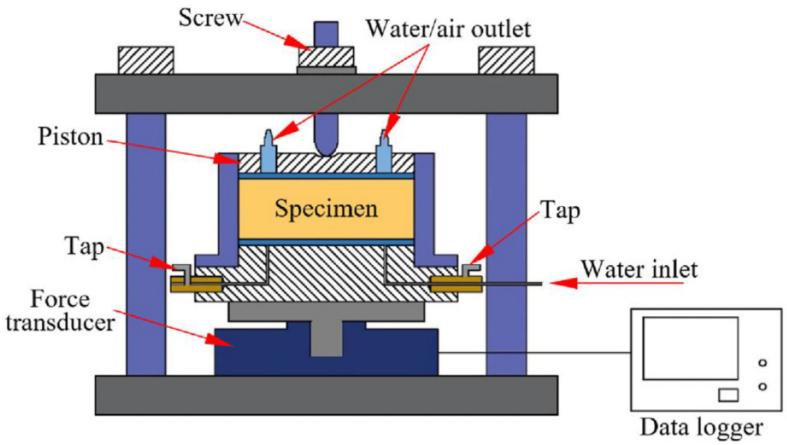

Table 3. Total suction measured using WP4.

Solution	Total suction (MPa)	Osmotic suction (MPa)	Stress release suction (MPa)
BC synthetic solution	3.5	0	3.5
Na = 60%; IS = 1.0 mol/L	5.0	0.75	4.25
Na = 90%; IS = 2.0 mol/L	9.0	4	5

of the injection pressure on the swelling pressure. Once the swelling pressure stabilized, the solution within the water/salt-solution converter was substituted with the next concentration solution, following the aforementioned protocol.

The saturated hydraulic conductivity, k_s (m/s), was calculated using Darcy's law

$$(3) \qquad k_s = \frac{\Delta Q}{A.i} = \frac{\Delta Q.l}{A.\Delta h} = \frac{\Delta Q.l}{A.(h_1 - h_2)} = \frac{\Delta Q.l}{A.(100 - 0)}$$

where ΔQ represents the inflow rate monitored by the CPV (m^3/s), A denotes the cross-sectional area of the test sample (m^2), i stands for the hydraulic gradient, l is the height of the sample (m), Δh signifies the difference in water head (m), h_1 corresponds to the water head at the inflow point, and h_2 refers to the water head at the outflow point. For example, if the water pressure applied at the inflow point was 1.0 MPa, h_1 was maintained at 100 m; h_2 was considered zero due to the presence of a thin layer of water at the outflow point.

3. Experimental results

3.1. Effect of solute concentration on swelling pressure

The impact of the solution concentration on the swelling pressure of BC is illustrated in Fig. 3. It appears that the stabilized swelling pressure decreased from 0.75 MPa (BC synthetic solution, 0.015 mol/L $NaHCO_3$) to 0.425 MPa (1.0 mol/L (Na, Ca)NO_3) and further to 0.29 MPa (2.0 mol/L (Na, Ca)NO_3). In other words, the swelling pressure of BC decreases with the increase in infiltration solution concentration. This finding aligns with the results reported by various researchers (Karnland et al. 2006; Castellanos et al. 2008; Herbert et al. 2008; Komime et al. 2009; Siddiqua et al. 2011; Lee et al. 2012). Moreover, the swelling pressure experiences a rapid initial growth during solution percolation and eventually stabilizes. The duration of the tests was defined by the time required for the swelling pressure to stabilize. A higher salt concentration led to a reduction of the swelling process duration. Specifically, the stabilization time was approximately 1 h for a concentration of 2.0 mol/L, and extended to 2 h for a concentration of 1.0 mol/L. In the case of BC synthetic solution, the evolution of swelling pressure achieved complete stabilization after 10 h. This phenomenon can primarily be attributed to the infiltration being driven by the matric suction gradient during primary swelling, and to the transportation of salts and cation exchange, which led to an increase in osmotic suction during the secondary swelling (Rao and Shivananda 2005). At higher concentrations, a more pronounced suction gradient is generated, due to the difference of the osmotic suction of injected solution (Table 3). This led to a lower swelling pressure.

3.2. Effect of sodium occupancy on swelling pressure

The impact of sodium occupancy on swelling pressure is illustrated in Figs. 4, 5, and 6. Figure 4 shows three duplicate swelling pressure tests (tests 1, 2, and 3), all with the same experimental procedure and infiltration solutions. It can be observed that as the sodium solution concentration increases from 1.0 to 2.0 mol/L while maintaining a constant sodium

Fig. 3. Evolution of the swelling pressures over time with different solute concentrations.

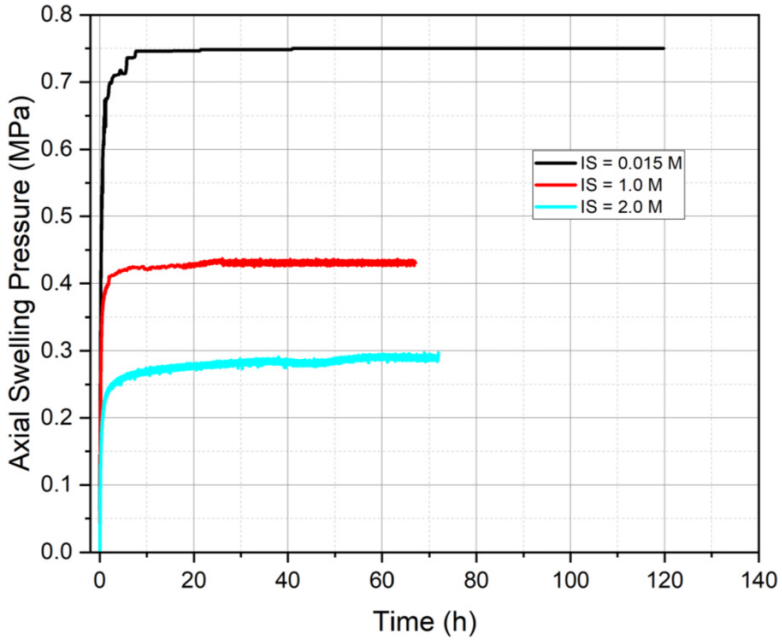

Fig. 4. Evolution of the swelling pressure of samples percolated with different saline solutions (Na = 60%—IS = 1.0 mol/L → Na = 60%—IS = 2.0 mol/L→ Na = 90%—IS = 2.0 mol/L). IS, ionic strength.

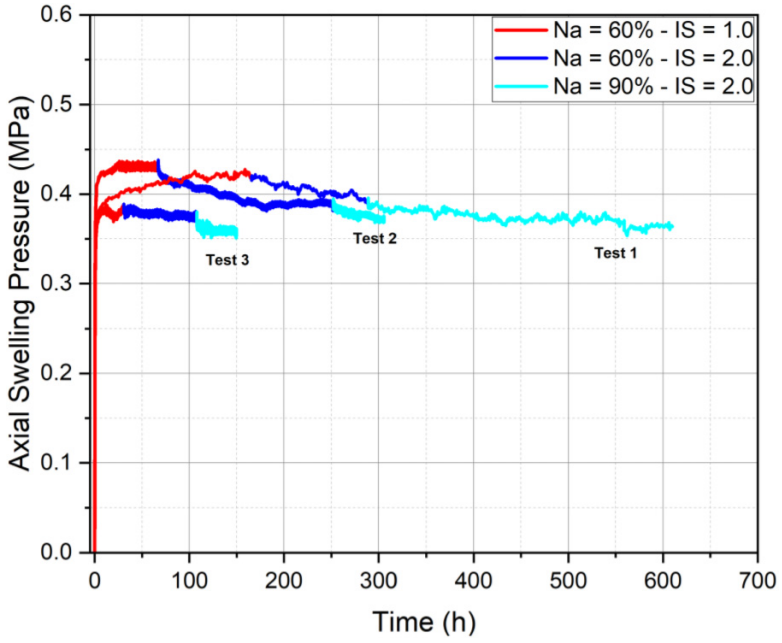

occupancy of 60%, the swelling pressure decreases. Subsequently, at 2.0 mol/L concentration, increasing the occupancy to 90% leads to a further reduction in the swelling pressure. Note that the close alignment of the three curves highlights the high repeatability of the results. Figure 5 shows the results of two additional swelling pressure tests (tests 4 and 5). The first test began with the percolation of BC synthetic solution, followed by an increase in concentration up to 1.0 mol/L with a 60% occupancy, resulting in a reduction of swelling pressure. Additionally, holding the sodium occupancy constant while increasing the solute concentration leads to a further decrease in swelling pressure. Likewise, when the sodium occupancy is increased at the same solution concentration, the swelling pressure continues to decrease, underlining the comparable influence of occupancy and concentration on the swelling pressure. Another pair of tests (tests 6 and 7) were initiated with higher solute concentration and sodium occupancy (90%–2.0 mol/L) (Fig. 6), and a decrease in both parameters revealed a very slight increase in swelling pressure. This slight increase of the swelling pressure might

Fig. 5. Evolution of the swelling pressure of samples percolated with different saline solutions (BC synthetic solution → Na = 60%—IS = 1.0 mol/L→ Na = 60%—IS = 2.0 mol/L→ Na = 90%—IS = 2.0 mol/L). BC, Boom Clay; IS, ionic strength.

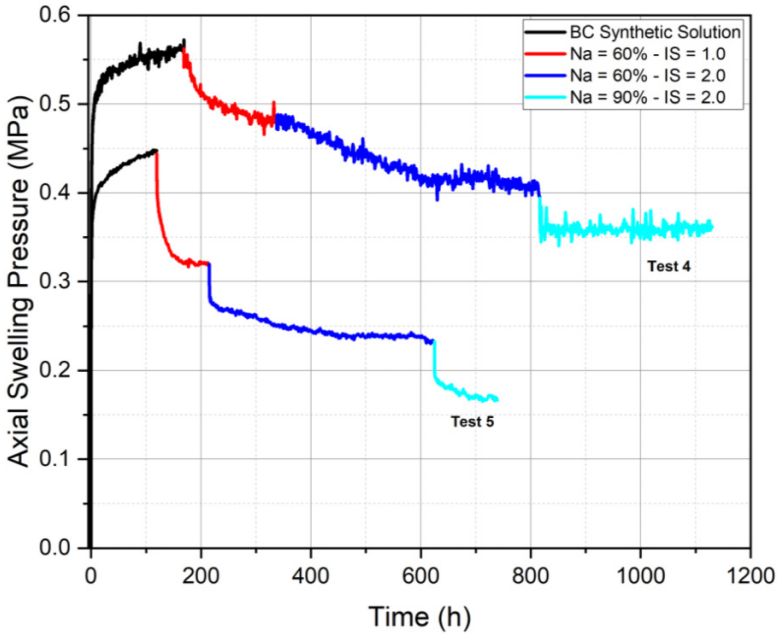

Fig. 6. Evolution of the swelling pressure of samples percolated with different saline solutions (Na = 90%—IS = 2.0 mol/L→ Na = 60%—IS = 2.0 mol/L→ Na = 60%—IS = 1.0 mol/L). IS, ionic strength.

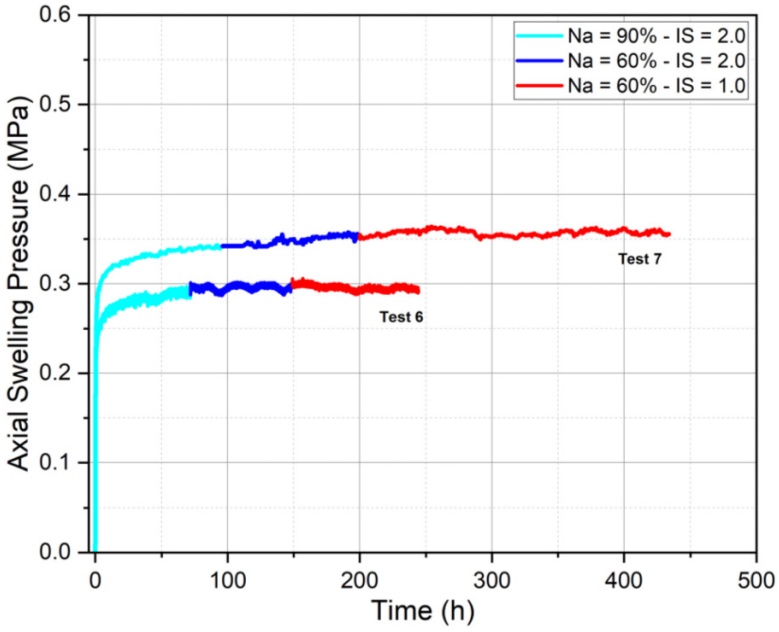

be explained by the larger number of pore volume replacements needed to establish a new equilibrium with decreasing solute concentration, rather than with increasing concentration. These results exhibit internal consistency: the swelling pressure decreases as sodium occupancy and solute concentration increase, while a slight increase in the swelling pressure was detected with decreasing solute concentration and sodium occupancy.

3.3. Effect of sodium occupancy and solute concentration on hydraulic conductivity

Figure 7 shows the impact of the concentration and occupancy of sodium, on the evolution of the hydraulic conductivity of BC samples that are consecutively equilibrated with the different solutions. At the outset, all samples were percolated with BC synthetic solution, yielding a value of K equal to 4.5×10^{-12} m/s, which aligns with the findings

Fig. 7. Evolution of hydraulic conductivity with varying sodium occupancy and solute concentration (BC synthetic solution → Na = 60%—IS = 1 mol/L → Na = 60%—IS = 2 mol/L → Na = 90%—IS = 2 mol/L). BC, Boom Clay; IS, ionic strength.

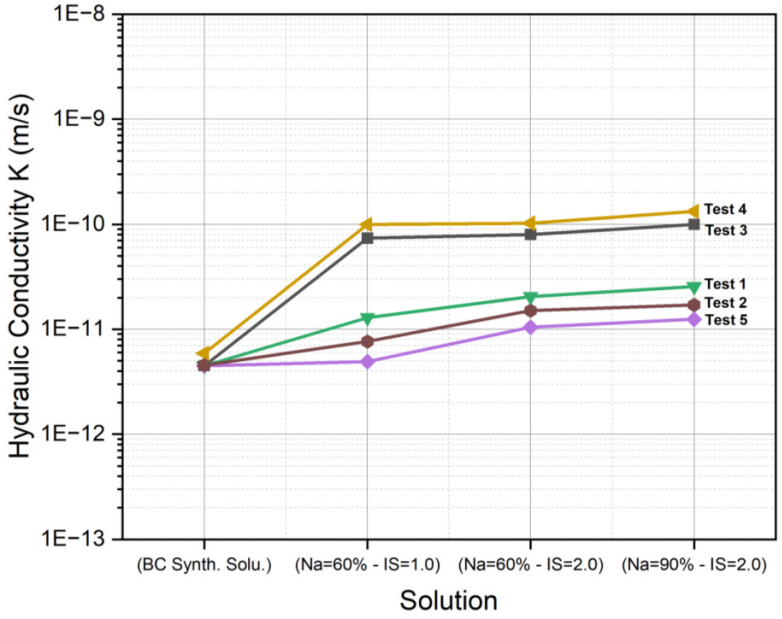

from existing literature (Horseman et al. 1987; Yu et al. 2013). In particular, the values for the hydraulic conductivity of BC reported in the literature under the field conditions (BC synthetic solution) varies from 1.5×10^{-12} to 4×10^{-12} (Wemaere et al. 2008). In this study, the highest recorded K value changes from 5.8×10^{-12} m/s (resulting from BC synthetic solution) to 9.9×10^{-11} m/s (using a 1.0 mol/L (Na, Ca)NO_3 solution with 60% Na^+ occupancy), and further to 1.03×10^{-10} m/s (with a 2.0 mol/L (Na, Ca)NO_3 solution, 60% Na^+ occupancy), and finally reaching 1.23×10^{-10} m/s (with a 2.0 mol/L $NaNO_3$ solution, 90% sodium occupancy). Interestingly, the hydraulic conductivity is positively correlated with the concentration of infiltrating sodium solutions. This observation is congruent with the findings reported by other researchers (Villar 2006; Chen et al. 2016), who explored the effects of saline and alkaline solutions on the hydraulic conductivity of MX-80 bentonite/granite mixture (with a ratio of 30/70 in dry mass) and GMZ01 bentonite, respectively. This pattern is also in agreement with the outcomes from various other studies. Karnland et al. (1992) identified an increase in permeability for compacted MX-80 bentonite by half an order of magnitude when permeant salinity was elevated from distilled water to 3.5 mol/L NaCl. Similarly, Villar (2005) highlighted a 135% higher hydraulic conductivity for compacted MX-80 bentonite when exposed to saline water (0.5 mol/L salinity) compared to de-ionized water. Castellanos et al. (2008) discovered these fluctuations to be comparable in scale to those observed in compacted FEBEX bentonite.

These results are not consistent with those presented in the study by Bleyen et al. (2018). These authors observed the evolution of hydraulic conductivity for a BC core (length = 3 cm, diameter = 3.8 cm) consecutively percolated with real BC pore water (RBCW) and with RBCW containing 0.1, 0.5, or 1 mol/L $NaNO_3$ over a total test duration of approximately 10 years. The percolation tests were conducted under oedometer conditions with a constant effective stress of 2.75 MPa.

It was observed that immediately after switching to a higher concentration (i.e., a higher IS), the hydraulic conductivity increased rapidly but slightly (by approximately 25%). Conversely, when Na^+ exchange occurred over longer time, the hydraulic conductivity began to decrease. this behaviour was attributed to the decrease in electrical diffuse layer thickness for the increase of the hydraulic conductivity. The effect was counteracted in the following weeks by $Na^+ - M^{2+}$ cation exchange processes and, to some extent, by the subsequent deterioration of the microstructure ("slaking") due to the ion exchange with sodium. Note that the test duration was almost 10 years, and it is known that the hydraulic conductivity of clay cores under continuous vertical stress decreases slowly with time (~10% after 6 years; N. Maes, SCK•CEN, personal communication, 2013), probably due to the creep of the clay. All this has to be kept in mind when interpreting the results of these tests and comparing them to the tests done in this work.

It is worth noting that in this study, the determination of hydraulic conductivity was instantaneous after directly switching to a higher solution concentration and sodium occupancy under constant volume condition, thereby representing the immediate hydraulic conductivity after such a switch. Furthermore, over time, the hydraulic conductivity of BC may decrease due to its self-sealing capacity, which can lead to the closure of some macropores. Further investigations are required to better understand such complex process.

4. Discussion

4.1. Effect of solute concentration on swelling pressure

Various studies showed that the swelling capacity of clayey material is lower in saline water; the higher the dissolved salt concentration, the lower the swelling pressure (Studds et al. 1998; Karnland et al. 2005, 2006; Suzuki et al. 2005; Castellanos et al. 2008; Katsumi et al. 2008; Siddiqua et al. 2011). The swelling behaviour of unsaturated soil upon exposure to water or electrolytes is commonly governed by two primary mechanisms: crystalline swelling and diffuse double-layer (DDL) swelling (Madsen and Müller-Von 1989; Savage 2005). Crystalline swelling is prompted by the hydration of initially dehydrated exchangeable cations (K^+, Na^+, Ca^{2+}, and Mg^{2+}) between the unit layers of montmorillonite. This mineral has a structure with a single alumina octahedral sheet enclosed between two silica tetrahedral sheets (TOT). The DDL swelling leads to more extensive and prolonged swelling, often referred to as long-term swelling. The swelling potential of expansive clays is influenced by factors such as overburden stress, unloading conditions, water exposure, and water content. The swelling characteristics of bentonite have been studied by various researchers. Evans and Quigley (1992) explored the effects of salt (copper solution) leaching from solid waste on permeability and swell percentage in sand–bentonite mixtures. They found that salt leaching increased permeability while decreasing swelling. Similarly, Simons and Reuter (1985) investigated the influence of salt leaching from waste and absorption, revealing changes in ions and electrostatic forces that led to the decrease in the swelling pressure and increase in the hydraulic conductivity. Di Maio (1996) observed an increase in free swelling of bentonite after interaction with water following exposure to NaCl, KCl, and $CaCl_2$ solutions. The exchange of Na^+ was found to be reversible, unlike the exchange of Ca^{2+} or K^+.

The results from this study illustrate a decrease in swelling pressure as sodium concentrations increase. This behaviour can be qualitatively explained by the DDL theory. On a mesoscopic scale (1–10 μm), the IS of the solution governs the repulsion forces between particles and influences osmotic pressure within micro-pores (0.01–1 μm) (Matuso 1977). As the cation concentration in the pore water increases, the thickness of the DDL and the repulsive force decrease (Mitchell and Soga 2005). Consequently, a lower swelling pressure was observed for the specimens percolated with saline solutions.

4.2. Effect of sodium occupancy on swelling pressure

For a specific type of clay, its structure is influenced by two main factors: (i) the ionic composition of the exchange complex and (ii) the pH level. The characteristics of the exchange complex are primarily affected by the valence, concentration, size, and hydration properties of the cations. Alterations in the chemical composition of the pore fluid bring about distinct impacts on clays. These changes might lead to cation exchanges between mineralogical units, variations of the electrochemical forces acting among different platelets, and variations in osmotic pressure. The cation exchange reaction is mainly controlled by the exchange capacity of the clay minerals (Mata 2003). The ease with which a cation of one type can replace a cation of another type depends mainly on the valence, relative abundance of the different cation types, and the cation size. On a microscopic scale (interlamellar space of montmorillonite sheets), the spacing between different unit layers is contingent upon the valence, dimensions, and hydration state of the interlayer cations. When the cations present in the pore water possess considerable replacing potential, cation exchange can occur, potentially altering the clay type. The commonly admitted competitive order is: $Na^+ < K^+ < Mg^{2+} < Ca^{2+}$ (Mata 2003; Mitchell and Soga 2005; Sun et al. 2018; Zeng et al. 2021*b*). Furthermore, high sodium concentrations in infiltrated saline solution samples may lead to the replacement of divalent ions, such as calcium, which tends to reduce the DDL. Alawaji (1999) also indicated that the swelling potential diminishes with elevated sodium concentration in the liquid composition.

Table 4. Hydrated radius of cations.

Cation	*Kielland (1937)*	*Mitchell and Soga (2005)*	*Lide and Frederikse (1995)*
Na^+	0.4–0.45 nm	0.56–0.79 nm	0.358 nm
K^+	0.3 nm	0.38–0.53 nm	0.331 nm
Mg^{2+}	0.8 nm	1.08 nm	0.628 nm
Ca^{2+}	0.6 nm	0.96 nm	0.812 nm
Al^{3+}	0.9 nm	–	–

Martens et al. (2011) performed a series of laboratory percolation experiments on undisturbed and saturated BC cores. RBCW and RCBW with additional $NaNO_3$ with concentrations up to 1 mol/L were injected in four steps into clay cores. The concentration of Na, K, Ca, Mg, and Sr in the eluted water were measured. It was found that after every switch of the $NaNO_3$ concentration, the concentration profiles of K, Ca, Mg, and Sr showed a sharp rise, followed by a slow decrease. It was also found that as a result of injecting high concentrations of sodium, the BC is transformed into Na-clay with almost 100% Na occupancy at exchange clay sites. Reactive coupled transport modelling with PHREEQC-2 was used to describe the experimentally observed elution curves for the cations. The model could fairly well describe the experimentally observed cation concentrations in the eluted water, confirming that cation exchange is indeed the dominant mechanism regulating the cation elution in the percolation experiments.

Infiltration of sodium cations into the interlayer spaces between montmorillonite sheets results in a decrease in swelling potential. This reduction could be attributed to the hydrated radius of the sodium cation. The adsorption of cations with varying hydrated radii by fine clayey soil emerges as a pivotal factor impacting swelling potential. The principal hydrated radii reported in the literature are presented in Table 4. Notably, sodium cations possess a smaller hydrated radius compared to calcium and magnesium. The

Fig. 8. Evolution of swelling pressure of a sample with Boom Clay (BC) synthetic solution and Na = 20%—IS = 1.0 mol/L. IS, ionic strength.

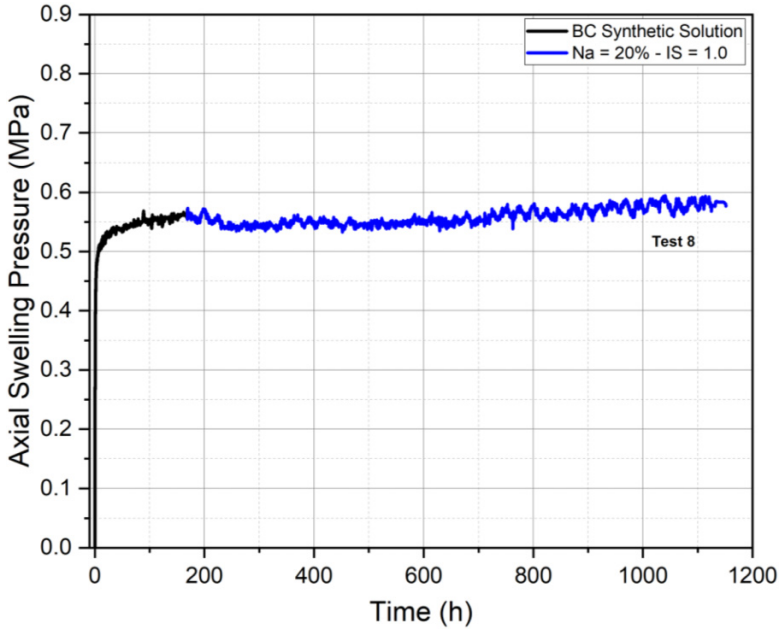

disparities among the hydrated radii presented in Table 4 may be attributed to the differing methods used to estimate the hydrated radius of each cation. The values provided by Mitchel and Soga (2005) were derived from the equations of Stern's theory as described by Olphen (1977), which account for both single and interacting flat double layers. These equations enable the calculation of charge within each layer and the potential at their interface. It is plausible that these variations are linked to the number of water molecule layers surrounding the cation, a quantity that likely varies depending on the scenarios, such as very low IS solutions, high IS solutions, or within the water layer in contact with a clay sheet in a dense clay matrix. The values of the hydrated radius given by Kielland (1937) were based on a revised and extended table of ionic activity coefficients, largely computed by independent means, taking into consideration the diameter of the hydrated ions as estimated by various methods. For sufficiently dilute solutions, the well-known Debye–Hückel formula was used. The effective diameters of the hydrated ions (noted as a_i) were approximately calculated by different methods, such as from the crystal radius and deformability according to the equation for cations given by Bonino (1933), or from the ionic mobilities or its empirical modification given by Young and Smith (2000). Sridharan et al. (1986) demonstrated that the hydrated cationic radius substantially affects the liquid limit of montmorillonite, a phenomenon more pronounced with monovalent cations than with higher valences.

Though limited data exists on the impact of the hydrated cationic radius on the swelling pressure of clays, it can be inferred that an increase in hydrated cationic radius results in a greater interlayer space, consequently yielding higher swelling capacity. Specifically, the hydrated radius of the Na^+ ion is approximately 10% larger than that of K^+, while it is approximately 30%–40% smaller than that of Mg^{2+} and Ca^{2+}.

To further investigate the influence of sodium occupancy on swelling pressure, two more tests with Na^+ occupancies of 10% and 20% were performed. The procedure started with the infiltration of the BC synthetic solution, followed by percolation involving a solution containing 1.0 mol/L solution concentration with 20% (Fig. 8) and 10% (Fig. 9) sodium occupancy, respectively. The solutions infiltrated into these samples are prepared by mixing sodium nitrate ($NaNO_3$) and calcium nitrate $Ca(NO_3)_2$, leading to an increase of calcium fraction in the solution due to the increase of the $Ca(NO_3)_2$ concentration.

The evolutions of swelling pressure with 20% and 10% Na occupancy are illustrated in Figs. 8 and 9, respectively. It is seen that the infiltration of the BC synthetic solution led to a swelling pressure of 0.6 and 0.75 MPa, respectively. This synthetic solution was maintained until two pore volume replacements were completed. The subsequent part of the graph can be divided into two phases: initially, there is a slight decrease in swelling pressure, followed by an increase. For the sample with 10% Na^+ occupancy a greater increase was observed compared to the 20% sample. The initial decrease in both cases align with the DDL theory and the compression of clay platelets along with the decreased thickness of the DDL. As infiltration continues with a solution containing fewer sodium cations and more calcium cations, the calcium cations, which have a larger hydrated radius than sodium cations, begin to replace the Na^+ cations situated within the interlayer space, triggering an increase in swelling pressure.

Fig. 9. Evolution of swelling pressure with Boom Clay (BC) synthetic solution and Na = 10%—IS = 1.0 mol/L. IS, ionic strength.

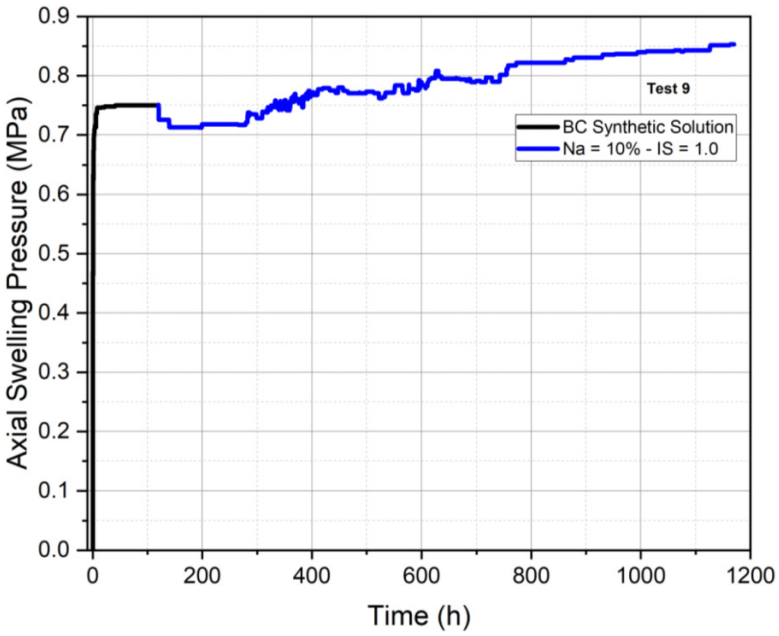

4.3. Effect of sodium occupancy and solute concentration on hydraulic conductivity

During the pore water replacement, it appears that higher concentrations of salt solution and sodium occupancy led to lower swelling pressure and higher hydraulic conductivity. According to Castellanos et al. (2008), several mechanisms may be at play, including alterations in pore size distribution due to the swelling of the clay matrix, and variations in water molecule mobility associated with exchangeable cations present on clay sheet surfaces (interlayer space) or within the DDL. As a result, an increase in salt concentration of the pore water leads to reduced swelling capacity of clay particles, thereby enlarging the size of larger flow channels (inter-aggregate) and subsequently increasing permeability.

Additionally, in this study, an increase in sodium occupancy leads to a decrease in swelling pressure and interlayer spacing between montmorillonite sheets, giving rise to the formation of more micro-fissures. This phenomenon could explain the observed increase in hydraulic conductivity with rising sodium occupancy. Conversely, a reduction in pore water salt concentration amplifies the development of the DDL, causing a decrease in permeability due to the decrease size of larger flow channels. In other words, aggregation of clay enlarges macro-pores as a consequence of increased pore water salt concentration, ultimately increasing soil permeability.

The influence of pore water salt concentration and occupancy on permeability remained consistent: higher concentrations or occupancy resulted in higher permeability. Numerous findings on compacted swelling clays demonstrated a correlation between pore water salinity and permeability increase. For instance, FEBEX bentonite exhibited a 184% rise in hydraulic conductivity with a NaCl concentration of 0.22 mol/L compared to distilled water. Similarly, with a NaCl concentration of 5.5 mol/L, the permeability coefficient doubled. MX-80 bentonite displayed a five to six-fold increase in K when shifting from distilled water to 3.5 mol/L NaCl, as confirmed by Karnland et al. (1992). Villar (2005) reported a 135% increase in K for MX-80 bentonite using a 0.5 mol/L NaCl solution in comparison to pure water. Experiments by Pusch (2001) exhibited a two-order of magnitude increase in K with a salinity rise from 0% to 20% on Friedland Ton clay, a natural clay containing 45% smectite. Furthermore, Castellanos et al. (2008) and Pusch (2001) concluded that sodium induces a greater increase in permeability than calcium.

5. Conclusion

One-dimensional swelling tests based on the constant-volume method were conducted on intact samples of the poorly indurated BC, which is considered as a potential host formation for the disposal of intermediate-level and high-level long-lived waste in Belgium. Mixed sodium and calcium nitrate solutions with total concentrations of 1.0 and 2.0 mol/L, coupled with varying target sodium occupancies of 10%, 20%, 60%, and 90%, were percolated through the samples. The BC synthetic solution of 15 mmol/L $NaHCO_3$ coupled with a Na^+ occupancy of ~30% served as a reference point. Throughout the test, axial swelling pressure was recorded by a force introducer sensor and hydraulic conductivity were determined, aiming to assess the impact of sodium concentrations and occupancies on the swelling behaviour and hydraulic conductivity of BC. The results lead to the following conclusions:

– A higher IS may reduce the swelling potential by contracting the DDL, in agreement with previous studies which indicated that a decrease in DDL thickness follows the collapse of clay structure brought about by salt solutions, leading to a reduction in swell potential.

- Cation exchange between saline solutions and the cations situated in the interlayer space of smectites could trigger the substitution of divalent cations, such as calcium, with monovalent cations like sodium. The decreased hydrated radius of the charge-balancing cation contributes to a decrease in swelling pressure.
- The outcomes illustrate that for fully saturated intact BC samples, infiltration of high-sodium concentration solutions, resulting in high Na^+ occupancies, initially led to a decrease in DDL (affecting the osmotic swelling), followed by a reduction in interlayer space (affecting the crystalline swelling). Conversely, percolation of solutions that result in a low sodium occupancy (10% and 20%) and high IS (1.0 mol/L) initially resulted in a decrease in swelling pressure related to DDL theory, followed by an increase in swelling pressure attributed to crystalline swelling, facilitated by the exchange of divalent cations, such as calcium, with monovalent cations, such as sodium.
- Any transition to a higher sodium concentration or occupancy immediately triggered a rise in hydraulic conductivity. This phenomenon might be connected to the reduced thickness of the DDL and the compression of interlayer spaces, fostering the creation of preferential pathways. These pathways lead to the formation of more accessible pores within the interparticle pore space, ultimately boosting the fraction of mobile water.

Article information

History dates

Received: 12 July 2024
Accepted: 16 December 2024
Accepted manuscript online: 18 December 2024
Version of record online: 20 February 2025

Copyright

Data availability

Data is available upon request.

Author information

Author ORCIDs

Yu-Jun Cui https://orcid.org/0000-0003-1886-3923
Frédéric Collin https://orcid.org/0000-0003-2220-7398

Author notes

Yu-Jun Cui served as Associate Editor at the time of manuscript review and acceptance; peer review and editorial decisions regarding this manuscript were handled by another editorial board member.

Author contributions

Conceptualization: YJC, XLL, SS, EV, LW, FC
Data curation: HAM
Formal analysis: HAM, YJC
Investigation: HAM, YJC, TG, FC
Methodology: HAM, YJC, XLL, EV, LW
Project administration: TG
Supervision: YJC, XLL, SS, EV, FC
Validation: LW, TG, FC
Writing – original draft: HAM
Writing – review & editing: YJC, SS, EV, TG

Competing interests

The authors declare that there is no conflict of interest.

References

Agus, S.S., Arifin, Y.F., Tripathy, S., and Schanz, T. 2013. Swelling pressure–suction relationship of heavily compacted bentonite–sand mixtures. Acta Geotechnica, **8**: 155–165.

Alawaji, H.A. 1999. Swell and compressibility characteristics of sand–bentonite mixtures inundated with liquids. Applied Clay Science, 411–430.

Awarkeh, M. 2023. Investigation of the long-term behaviour of Boom Clay (Doctoral dissertation, Marne-la-vallée, ENPC).

Barshad, I. 1952. Factors affecting the interlayer expansion of vermiculite and montmorillonite with organic substances. Soil Science Society of America Journal, **16**: 176–182. doi:10.2136/sssaj1952.03615995001600020018x.

Bergaya, F., and Vayer, M. 1997. CEC of clays: measurement by adsorption of a copper ethylenediamine complex. Applied Clay Science, **12**: 275–280. doi:10.1016/S0169-1317(97)00012-4.

Bethke, C.M., Farrell, B., and Sharifi, M. 2021. The Geochemist's Workbench® Release 16 (Five Volumes). Aqueous Solutions LLC, Champaign, Illinois.

Beyer, R., and Steiger, M. 2002. Vapour pressure measurements and thermodynamic properties of aqueous solutions of sodium acetate. The Journal of Chemical Thermodynamics, **34**(7): 1057–1071. doi:10.1006/jcht.2002.0974.

Blanc, P., Lassin, A., Piantone, P., Azaroual, M., Jacquemet, N., Fabbri, A., and Gaucher, E.C. 2012. Thermoddem: a geochemical database focused on low temperature water/rock interactions and waste materials. Applied Geochemistry, **27**(10): 2107–2116. doi:10.1016/j.apgeochem.2012.06.002.

Bleyen, N., Mariën, A., and Valcke, E. 2018. The geochemical perturbation of Boom Clay due to the $NaNO_3$ plume released from Eurobitum bituminised radioactive waste: status 2013. External Report. SCK-CEN, Mol, Belgium. SCK• CEN-ER-221.

Bolt, G.H. 1956. Physico-chemical analysis of the compressibility of pure clays. Géotechnique, **6**: 86–93. doi:10.1680/geot.1956.6.2.86.

Bonino, G.B. 1933. Grant, J.-The Measurement Of Hydrogen Ion Concentration.

Calvello, M., Lasco, M., Vassallo, R., and Di Maio, C. 2005. Compressibility and residual shear strength of smectitic clays: influence of pore aqueous solutions and organic solvents. (Vol. 13). Italian Geotechnical Journal, **1**(2005): 34–46.

Castellanos, E., Villar, M.V., Romero, E., Lloret, A., and Gens, A. 2008. Chemical impact on the hydro-mechanical behaviour of high-density FEBEX bentonite. Physics and Chemistry of the Earth, Parts A/B/C, **33**: S516–S526. doi:10.1016/j.pce.2008.10.056.

Chapman, N., and Hooper, A. 2012. The disposal of radioactive wastes underground. Proceedings of the Geologists' Association, **123**(1)46–63. doi:10.1016/j.pgeola.2011.10.001.

Chen, Y.G., Zhu, C.M., Ye, W.M., Cui, Y.J., and Chen, B. 2016. *Effects of solution concentration and vertical stress on the swelling behavior of compacted GMZ01 bentonite*. (Vol. 10). Applied Clay Science, **124-125**: 11–20. doi:10.1016/j.clay.2016.01.050.

De Craen, M., Wang, L., Van Geet, M., and Moors, H. 2004. Geochemistry of Boom Clay pore water at the Mol site. SCK-CEN Scientific Report BLG-990. Waste & Disposal Department SCK-CEN, Mol, Belgium.

Di Maio, C. 1996. Exposure of bentonite to salt solution: osmotic and mechanical effects. Géotechnique,**46**: 695–707. doi:10.1680/geot.1996.46.4.695.

Di Maio, C., Santoli, L., and Schiavone, P. 2004. Volume change behaviour of clays: the influence of mineral composition, pore fluid composi-

tion and stress state. (Vol. 17). Mechanics of Materials, **36**(5-6): 435–451. doi:10.1016/S0167-6636(03)00070-X.

Du, J., Zhou, A., Lin, X.B., and Kodikara, J. 2021. Prediction of swelling pressure of expansive soil using an improved molecular dynamics approach combining diffuse double layer theory. Applied Clay Science, **203**: 105998. doi:10.1016/j.clay.2021.105998.

Evans, E.A., and Quigley, R.M. 1992. Permeation of sand-bentonite mixtures with municipal waste leachate. Geotechnical Research Centre, University of Western Ontario.pp. 68/1–68/8.

Frederickx, L., Honty, M., Craen, M.D., Dohrmann, R., and Elsen, J. 2018. Relating the cation exchange properties of the Boom Clay (Belgium) to mineralogy and pore-water chemistry. Clays and Clay Minerals, **66**(5): 449–465. doi:10.1346/CCMN.2018.064111.

Frederickx, L., Honty, M., De Craen, M., and Elsen, J. 2021. Evaluating the quantification of the clay mineralogy of the Rupelian Boom Clay in Belgium by a detailed study of size fractions. Applied Clay Science, **201**: 105954. doi:10.1016/j.clay.2020.105954.

Herbert, H.J., Kasbohm, J., Sprenger, H., Fernández, A.M., and Reichelt, C. 2008. Swelling pressures of MX-80 bentonite in solutions of different ionic strength. Physics and Chemistry of the Earth, Parts A/B/C, **33**: S327–S342. doi:10.1016/j.pce.2008.10.005.

Honty, M. 2010. CEC of the Boom Clay–a review. SCK-CEN report ER-134.

Honty, M., Frederickx, L., Wang, L., De Craen, M., Thomas, P., Moors, H., and Jacops, E. 2022. Boom Clay pore water geochemistry at the Mol site: experimental data as determined by in situ sampling of the piezometers. Applied Geochemistry, **136**: 105156. doi:10.1016/j.apgeochem.2021.105156.

Horseman, S.T., Winter, M.G., and Enwistle, D.C. 1987. Geotechnical characterization of Boom Clay in relation to the disposal of radioactive waste.

Karnland, O., Nilsson, U., Olsson, S., and Sellin, P. 2005. Experimental study on sealing properties of commercial bentonites related to bentonite mineralogy and water solution composition.

Karnland, O., Olsson, S., and Nilsson, U. 2006. Mineralogy and sealing properties of various bentonites and smectite-rich clay materials (No. SKB-TR—06-30). Swedish Nuclear Fuel and Waste Management Co.

Karnland, O., Pusch, R., and Sandén, T. 1992. The importance of electrolyte on the physical properties of MX-80 bentonite. Stockholm, Sweden. Report AR, 92–35: Swedish Nuclear Fuel and Waste Management Company (SKB International AB).

Katsumi, T., Ishimori, H., Onikata, M., and Fukagawa, R. 2008. Long-term barrier performance of modified bentonite materials against sodium and calcium permeant solutions. Geotextiles and Geomembranes, **26**(1): 14–30. doi:10.1016/j.geotexmem.2007.04.003.

Kielland, J. 1937. Individual activity coefficients of ions in aqueous solutions. Journal of the American Chemical Society, **59**: 1675–1678. doi:10.1021/ja01288a032.

Komine, H., Yasuhara, K., and Murakami, S. 2009. Swelling characteristics of bentonites in artificial seawater. Canadian Geotechnical Journal, **46**: 177–189. doi:10.1139/T08-120.

Le, T.T., Cui, Y.J., Muñoz, J.J., Delage, P., Tang, A.M., and Li, X.L. 2011. Studying the stress-suction coupling in soils using an oedometer equipped with a high capacity tensiometer. Frontiers of Architecture and Civil Engineering in China, **5**: 160–170. doi:10.1007/s11709-011-0106-x.

Lee, J.O., Lim, J.G., Kang, I.M., and Kwon, S. 2012. Swelling pressures of compacted Ca-bentonite. Engineering Geology, **129-130**: 20–26. doi:10.1016/j.enggeo.2012.01.005.

Li, X.L., Van Geet, M., Bruggeman, C., and De Craen, M. 2023. Geological disposal of radioactive waste in deep clay formations: 40 years of RD&D in the Belgian URL HADES (No. 536). *Edited by* X.L. Li, M. Van Geet, C. Bruggeman and M. De Craen. (2023). Geological disposal of radioactive waste in deep clay formations: 40 years of RD&D in the Belgian URL HADES (No. 536). Geological Society of London Special Publications.

Lide, D.R., and Frederikse, H.P. 1995. CRC handbook of chemistry and physics . CRC Press. Inc, Boca Raton, FL.

Low, P.F. 1980. The swelling of clay: II. Montmorillonites. Soil Science Society of America Journal, **44**:667–676. doi:10.2136/sssaj1980.03615995004400040001x.

Madsen, F.T., and Müller-Vonmoos, M. 1989. The swelling behaviour of clays. Applied Clay Science, **4**: 143–156. doi:10.1016/0169-1317(89)90005-7.

Martens, E., Jacques, D., Wang, L., De Cannière, P., Van Gompel, M., Mariën, A., and Valcke, E. 2011. Modelling of cation concentrations in the outflow of $NaNO_3$ percolation experiments through Boom Clay cores. Physics and Chemistry of the Earth, Parts A/B/C, **36**(17-18): 1693–1699. doi:10.1016/j.pce.2011.07.021.

Mata Mena, C. 2003. Hydraulic behaviour of bentonite based mixtures in engineered barriers: the backfill and plug test at the Äspö HRL (Sweden). Universitat Politècnica de Catalunya.

Matsuo, S. 1977. Microscopic study on deformation and strength characteristics of clay soil. *In* Proceeding of the 9th International Conference SMFE. pp. 201–204.

McCombie, C. 2005. Geological disposal: global status and key issues. Practice periodical of hazardous, toxic, and radioactive waste management.

Mesri, G., and Olson, R.E. 1971. Mechanisms controlling the permeability of clays. Clays and Clay minerals, **19**: 151–158.

Mitchell, J.K., and Soga, K. 2005. Fundamentals of soil behavior. John Wiley & Sons, New York.

Mokni, N. 2011. Deformation and flow driven by osmotic processes in porous materials. Universitat Politècnica de Catalunya.

Olphen, H.V. 1977. An introduction to clay colloid chemistry, for clay technologists, geologists, and soil scientists. (2nd edition, p.318pp.)

Pusch, R. 2001. Experimental study of the effect of high porewater salinity on the physical properties of a natural smectitic clay. (Vol. 32).

Push, R. 2008. Geological storage of radioactive waste Berlin Heidelberg. **379**, Springer Verlag, Berlin, Heidelberg.

Rao, S.M., and Shivananda, P. 2005. Role of osmotic suction in swelling of salt-amended clays. Canadian Geotechnical Journal, **42**: 307–315. doi:10.1139/t04-086.

Rao, S.M., and Thyagaraj, T. 2007. Swell–compression behaviour of compacted clays under chemical gradients. Canadian Geotechnical Journal, **44**: 520–532. doi:10.1139/t07-002.

Savage, D. 2005. The effects of high salinity groundwater on the performance of clay barriers. Nottingham NG2 6FS: SKI.

Schanz, T., and Tripathy, S. 2009. Swelling pressure of a divalent-rich bentonite: Diffuse double-layer theory revisited. Water Resources Research **45**(5),10.1029/2007WR006495.

Siddiqua, S., Baltz, J., and Siemens, G. 2011. Evaluation of the impact of pore fluid chemistry on the hydromechanical behaviour of clay-based sealing materials. Canadian Geotechnical Journal, **48**: 199–213. doi:10.1139/T10-064.

Simons, H., and Reuter, E. 1985. Physical and chemical behaviour of clay-based barriers under percolation with test liquids. Engineering Geology, **21**: 301–310. doi:10.1016/0013-7952(85)90020-1.

Sposito, G. 1981. The thermodynamics of soil solutions. Oxford University Press.

Sridharan, A., and Rao, G.V. 1973. Mechanisms controlling volume change of saturated clays and the role of the effective stress concept. Géotechnique, **23**: 359–382. doi:10.1680/geot.1973.23.3.359.

Sridharan, A., Rao, S.M., and Murthy, N.S. 1986. Compressibility behaviour of homoionized bentonites. Géotechnique, **36**(4): 551–564. doi:10.1680/geot.1986.36.4.551.

Srodon, J., and McCarty, D.K. 2008. Surface area and layer charge of smectite from CEC and EGME/H2O-retention measurements. Clays and Clay Minerals, **56**: 155–174. doi:10.1346/CCMN.2008.0560203.

Studds, P.G., Stewart, D.I., and Cousens, T.W. 1998. The effects of salt solutions on the properties of bentonite-sand mixtures. Clay Minerals, **33**: 651–660. doi:10.1180/claymin.1998.033.4.12.

Sun, Z., Chen, Y.G., Cui, Y.J., Xu, H.D., Ye, W.M., and Wu, D.B. 2018. Effect of synthetic water and cement solutions on the swelling pressure of compacted Gaomiaozi (GMZ) bentonite: the Beishan site case, Gansu, China. Engineering Geology, **244**: 66–74. doi:10.1016/j.enggeo.2018.08.002.

Suzuki, S., Prayongphan, S., Ichikawa, Y., and Chae, B.G. 2005. In situ observations of the swelling of bentonite aggregates in NaCl solution. Applied Clay Science, **29**: 89–98. doi:10.1016/j.clay.2004.11.001.

Valcke, E., Marien, A., and Van Geet, M. 2009. The methodology followed in Belgium to investigate the compatibility with geological disposal of eurobitum bituminized intermediate-level radioactive waste. MRS Proceedings, **1193**: 105. doi:10.1557/PROC-1193-105.

Villar, M.V. 2005. MX-80 bentonite. Thermal–Hydro-mechanical Characterisation Performed at CIEMAT in the Context of the Prototype Project. Centro de Investigaciones Energeticas, Medioambientales y Tecnologicas (CIEMAT), Madrid (Spain).

Villar, M.V. 2006. Infiltration tests on a granite/bentonite mixture: influence of water salinity. Applied Clay Science, **31**: 96–109. doi:10.1016/j.clay.2005.07.007.
Wang, L., Honty, M., De Craen, M., and Frederickx, L. 2023. Boom Clay pore-water geochemistry at the Mol site: chemical equilibrium constraints on the concentrations of major elements. Applied Geochemistry, **148**: 105541. doi:10.1016/j.apgeochem.2022.105541.
Weetjens, E., E., and Mariën, A. 2010. Sodium nitrate release from EUROBITUM bituminised radioactive waste-scoping calculations. SCK CEN reports (ER-146).
Wemaere, I., Marivoet, J., and Labat, S. 2008. Hydraulic conductivity variability of the Boom Clay in north-east Belgium based on four core drilled boreholes. Physics and Chemistry of the Earth, Parts A/B/C, **33**: S24–S36. doi:10.1016/j.pce.2008.10.051.
Yang, J.W., Cui, Y.J., Mokni, N., and Wang, H. 2024. A triple-microstructure hydro-mechanical constitutive damage model for compacted MX80 bentonite pellet/powder mixture. International Journal for Numerical and Analytical Methods in Geomechanics.
Ye, W.M., Zheng, Z.J., Chen, B., Chen, Y.G., Cui, Y.J., and Wang, J. 2014. Effects of pH and temperature on the swelling pressure and hydraulic conductivity of compacted GMZ01 bentonite. Applied Clay Science, **7**.
Ying, Z., Cui, Y.J., Duc, M., Benahmed, N., Bessaies-Bey, H., and Chen, B. 2021. Salinity effect on the liquid limit of soils. Acta Geotechnica, **16**(4): 1101–1111.
Yotsuji, K., Tachi, Y., Sakuma, H., and Kawamura, K. 2021. Effect of interlayer cations on montmorillonite swelling: comparison between molecular dynamic simulations and experiments. Applied Clay Science, **204**: 106034. doi:10.1016/j.clay.2021.106034.
Young, D.A., and Smith, D.E. 2000. Simulations of clay mineral swelling and hydration: Dependence upon interlayer ion size and charge. The Journal of Physical Chemistry B, **104**(39): 9163–9170. doi:10.1021/jp000146k.
Yu, L., Rogiers, B., Gedeon, M., Marivoet, J., De Craen, M., and Mallants, D. 2013. A critical review of laboratory and in-situ hydraulic conductivity measurements for the Boom Clay in Belgium. Applied Clay Science, **75-76**: 1–12. doi:10.1016/j.clay.2013.02.018.
Yukselen-Aksoy, Y., Kaya, A., and Ören, A.H. 2008. Seawater effect on consistency limits and compressibility characteristics of clays. (Vol. 8). Engineering Geology, **102**(1-2): 54–61. doi:10.1016/j.enggeo.2008.07.005.
Zeng, Z., Cui, Y.J., and Talandier, J. 2021. Long-term effect of water chemistry on the swelling pressure and hydraulic conductivity of compacted claystone/bentonite mixture with technological gaps. Engineering Geology.
Zeng, Z., Cui, Y.J., Zhang, F., Conil, N., and Talandier, J. 2019. Investigation of swelling pressure of bentonite/claystone mixture in the full range of bentonite fraction. Applied Clay Science, **178**: 105137. doi:10.1016/j.clay.2019.105137.
Zhang, F., Cui, Y.J., and Chen, B. 2022. Investigation of suction effects due to stress release with compacted MX80 bentonite. Journal of Geotechnical and Geoenvironmental Engineering, **148**(9): 04022070. doi:10.1061/(ASCE)GT.1943-5606.0002849.
Zhu, C.M., Ye, W.M., Chen, Y.G., Chen, B., and Cui, Y.J. 2013. Influence of salt solutions on the swelling pressure and hydraulic conductivity of compacted GMZ01 bentonite. Engineering Geology, **7**.

Appendix A

Equilibrium calculations to estimate the amount of pore volumes of inlet water with given sodium and calcium concentrations to allow a Boom Clay (BC) core to reach a high sodium cation exchange occupancy (Na^+)

Computer code and the thermochemical database

The computer code used in this study is *The Geochemist's Workbench* (GWB) (Bethke et al. 2021). GWB is a software package designed for geochemical modeling, including equilibrium, kinetic, biochemical, and reactive transport calculations in 1D and 2D.

The thermochemical database employed is the Thermoddem database (Blanc et al. 2012), version V1.10_15Dec2020, available at https://thermoddem.brgm.fr/.

Chemical model and input data

The chemical model consists of the clay composition and the pore water composition in equilibrium with the clay. The clay component is a simplified representation of the BC mineral composition as determined by mineralogical studies (Frederickx et al. 2021). The current reference chemical model of BC is based on the study by Wang et al. (2023). The mineral assemblage representing the chemical properties of BC consists of seven minerals: quartz, kaolinite, chlorite, calcite, dolomite, siderite, and pyrite. This assemblage, when equilibrated with the pore water, accurately explains the observed characteristics of in situ pore water sampled at the Mol site in Belgium. The experimental water sampling and composition analysis were reported by Honty et al. (2022). Cation exchange properties of BC is also in the model and the data concerning selectivity, cation exchange capacity (CEC), cation occupancies are from the study of Frederickx et al. (2018).

For the equilibrium calculations, one liter of pore water, i.e., one pore volume, is put in equilibrium with CEC equivalent to 4 kg of clay, so mimicking the porosity of 20 wt.%. In other words, since BC has a CEC of 22.2 cmol/kg (Frederickx et al. 2018), the model clay has 4×0.22 eq $= 0.88$ eq CEC in the system.

Three scenarios are put forward to condition the clay core to reach the desired Na occupancy:

1. 2 mol/L $NaNO_3$ to reach 90% Na occupancy;
2. 1 mol/L $NaNO_3$ to reach 90% Na occupancy;
3. 1 mol/L ionic strength with 856 meq/L $NaNO_3$ and 144 meq $Ca(NO_3)_2$ to reach 60% Na occupancy.

GWB inputs were configured to "react" the three given inlet waters with the model clay, which includes clay minerals, cation exchange sites, and the initial BC pore water in the first pore volume (pv) of water. Reaction path calculations were performed using the "flush" model configuration, allowing the inlet water to interact with the model system and gradually displace the original pore water. This process continued step by step until the model clay achieved the desired sodium occupancy.

Results

Figures A1–A3 show the results of equilibrium calculations for three inlet solutions. The key observations are summarized as follows:

1. Approximately 4.5 pore volumes (pv) of 2 mol/L $NaNO_3$ are required to achieve 90% sodium occupancy in the clay core.
2. Approximately 10 pv of 1 mol/L $NaNO_3$ are needed to reach 90% sodium occupancy in the clay core.
3. Approximately 2.6 pv of a solution containing 856 meq/L $NaNO_3$ and 72 mmol/L $Ca(NO_3)_2$ are needed to achieve 60% sodium occupancy in the clay core.

Fig. A1. Cation exchange occupancies as function of displacement of pore volumes of inlet pore waters. Inlet concentrations: high ionic strength: 2 mol/L $NaNO_3$.

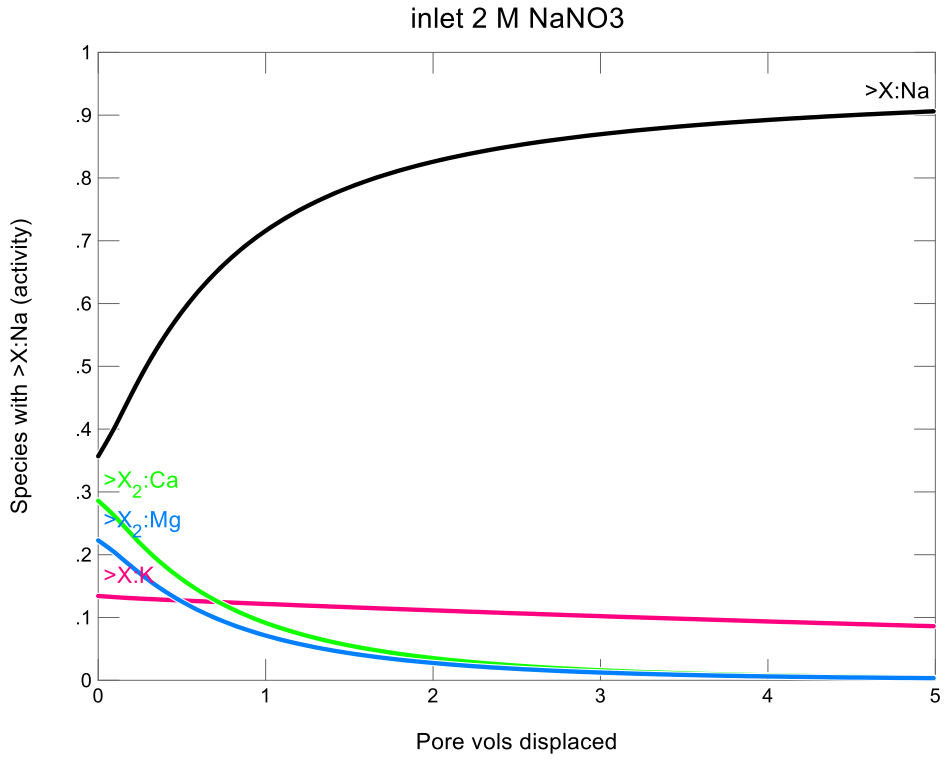

Fig. A2. Cation exchange occupancies as function of displacement of pore volumes of inlet pore waters. Inlet concentrations: medium ionic strength: 1 mol/L $NaNO_3$.

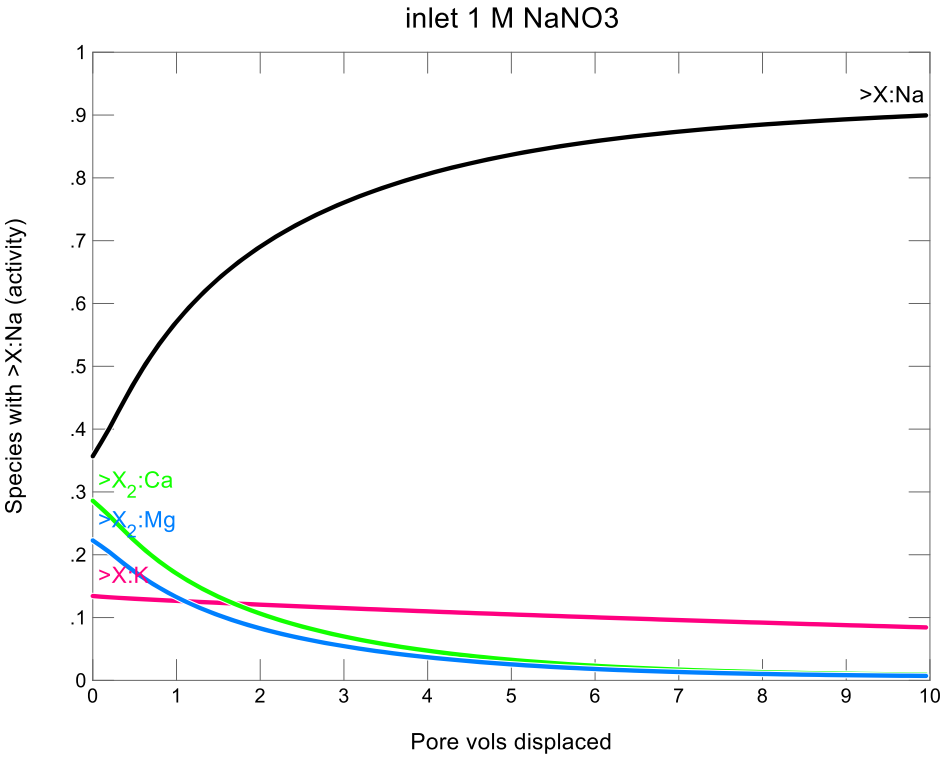

Fig. A3. Cation exchange occupancies as function of displacement of pore volumes of inlet pore waters. Inlet concentrations: medium ionic strength: 856 meq/L $NaNO_3$ and 72 mmol/L $Ca(NO_3)_2$.